

Cooperative Asymmetric Catalysis with Dimeric Salen Complexes

Reed G. Konsler, Jörn Karl, and Eric N. Jacobsen*

Department of Chemistry and Chemical Biology
Harvard University
Cambridge, Massachusetts 02138

Received July 28, 1998

Cooperative reactivity between multiple metal centers is commonly postulated for enzymatic systems¹ and has evolved into an intriguing design principle for synthetic catalysts.² We reported recently that the asymmetric ring opening (ARO) of meso epoxides with TMS-N₃ catalyzed by (salen)Cr complex **1**³ displays a second-order kinetic dependence on catalyst.⁴ This observation led to a mechanistic proposal for the ARO involving simultaneous activation of epoxide and azide by two different catalyst molecules (Figure 1). We have undertaken the design of catalysts that enforce this cooperative mechanism through the construction of covalently linked dimeric complexes, and we describe here the synthesis and successful application of such systems as highly enantioselective and efficient ARO catalysts. Kinetic and enantioselectivity data provide unambiguous evidence for a mechanism involving cooperative, intramolecular bimetallic catalysis.

A principal consideration in the design of dimeric analogues of **1** is the question of how to link the two salen units such that cooperative reactivity is favored. Two limiting geometries can be envisioned for the optimal selectivity-determining transition state, one a “head-to-head” alignment, and another in which one salen unit is rotated 180° relative to the other in a “head-to-tail” manner (Figure 2). Evaluation of a favored “head-to-head” orientation was approached through the synthesis of complex **2** and its monomeric analogue **3**.⁵ Complex **2** catalyzed the ARO of cyclopentene oxide with TMSN₃ with enantioselectivity comparable to that obtained with complex **1** (90% ee with **3**, vs 93% ee with **1**). In contrast, dimeric complex **2** effected the ARO with an accelerated rate relative to **3** but only 8% ee.⁶ Thus, linking the two salen units through the diimine backbone appeared to induce a cooperative mechanism, albeit through a far less enantiodiscriminating transition state than that attained with the monomeric catalysts.

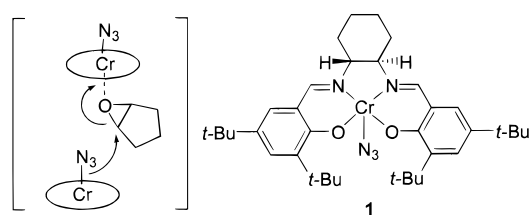


Figure 1. Proposed mechanism of cooperative bimetallic ARO of cyclopentene oxide catalyzed by **1**.

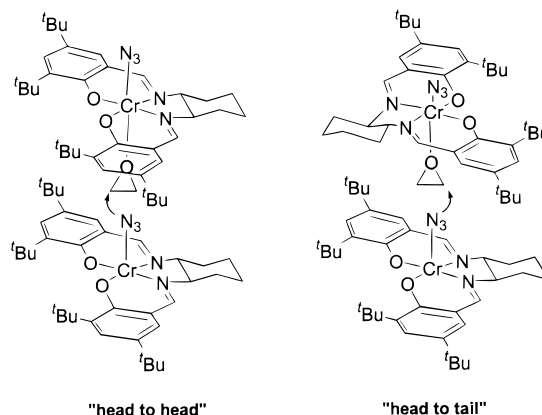
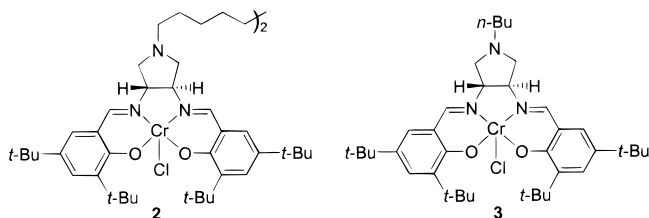
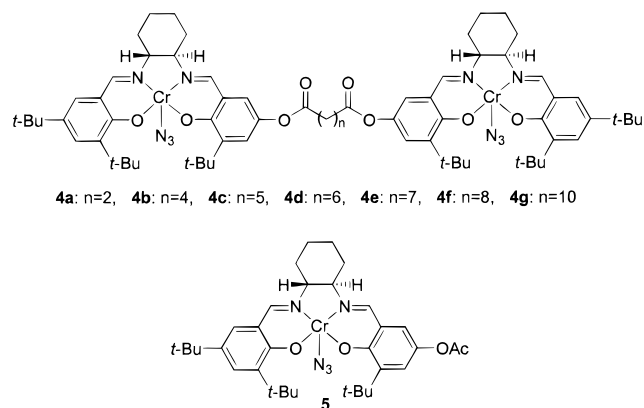


Figure 2. Two limiting geometries for the enantioselectivity-determining transition state of the ARO catalyzed by **1**.



In light of these results, the dimeric complexes were redesigned in order to allow intramolecular reaction through a greater range of transition state geometries. Dimeric complexes **4a–g** were synthesized along with the monomeric analogue **5**.⁵ Complexes



4a–g were found to catalyze the ARO of cyclopentene oxide by TMS-N₃ at concentrations an order of magnitude below the lower limit of reactivity for the monomeric complexes **1** and **5**⁷ while still yielding epoxide ring-opened product with comparable enantiopurity (Table 1).

Kinetic studies of the reaction of cyclopentene oxide with HN₃⁴ catalyzed by **1–5** were carried out by monitoring initial rates of

(1) For reviews: (a) Sträter, N.; Lipscomb, W. N.; Klabunde, T.; Krebs, B. *Angew. Chem., Int. Ed. Engl.* **1996**, *35*, 2024. (b) Wilcox, D. E. *Chem. Rev.* **1996**, *96*, 2435. (c) Steinhagen, H.; Helmchen, G. *Angew. Chem., Int. Ed. Engl.* **1996**, *35*, 2339.

(2) Representative examples: (a) Young, M. J.; Chin, J. *J. Am. Chem. Soc.* **1995**, *117*, 10577. (b) Molenveld, P.; Kapsabelis, S.; Engbersen, J. F. J.; Reinhoudt, D. N. *J. Am. Chem. Soc.* **1997**, *119*, 2948. (c) Vance, D. H.; Czarnik, A. W. *J. Am. Chem. Soc.* **1993**, *115*, 12165. (d) Matthews, R. C.; Howell, D. K.; Peng, W.-J.; Train, S. G.; Treleaven, W. D.; Stanley, G. G. *Angew. Chem., Int. Ed. Engl.* **1996**, *35*, 2253. (e) Liu, S.; Luo, Z.; Hamilton, A. D. *Angew. Chem., Int. Ed. Engl.* **1997**, *36*, 2678. (f) Sawamura, M.; Sudoh, M.; Ito, Y. *J. Am. Chem. Soc.* **1996**, *118*, 3309. (g) Chapman, W. H.; Breslow, R. *J. Am. Chem. Soc.* **1995**, *117*, 5462. (h) Ritter, J. C. M.; Bergman, R. G. *J. Am. Chem. Soc.* **1998**, *120*, 6826. (i) Arai, T.; Yamada, Y. M. A.; Yamamoto, N.; Sasai, H.; Shibasaki, M. *Chem. Eur. J.* **1996**, *2*, 1368, and references therein.

(3) Martínez, L. E.; Leighton, J. L.; Carsten, D. H.; Jacobsen, E. N. *J. Am. Chem. Soc.* **1995**, *117*, 5897.

(4) Hansen, K. B.; Leighton, J. L.; Jacobsen, E. N. *J. Am. Chem. Soc.* **1996**, *118*, 10924.

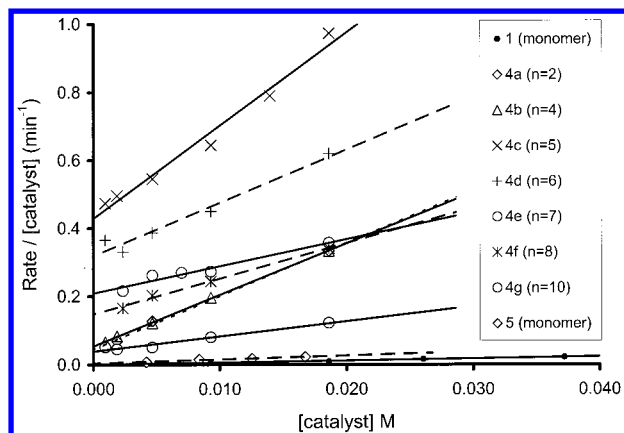
(5) Details of the synthesis and characterization of catalysts **2–5** may be found in the Supporting Information.

(6) Kinetic experiments analogous to those described for **4a–g** (Figure 3) indicated that, at the concentration studied ($[2] = 1 \times 10^{-3}$ M), complex **2** catalyzed the ARO primarily through a first-order pathway. At higher $[2]$, enantioselectivities in the ARO improved as a result of participation of a pathway that is second order in the dimer. For example, with $[2] = 2 \times 10^{-2}$ M, the ARO product was obtained in 86% ee.

Table 1. Rate Constants and Enantioselectivity Data for the Ring Opening of Cyclopentene Oxide Catalyzed by (salen)Cr–N₃ Complexes

catalyst	<i>n</i>	% ee of product ^a	<i>k</i> _{intra} (min ⁻¹ × 10 ⁻²) ^b	<i>k</i> _{inter} (M ⁻¹ min ⁻¹) ^b	<i>M</i> _{eff} (M × 10 ⁻³) ^b
1		93		0.6	
5		94		1.2	
4a	2	90	4.4	15.7	2.8
4b	4	90	5.4	15.1	3.6
4c	5	93	42.9	27.4	15.7
4d	6	93	31.7	15.8	20.1
4e	7	93	20.9	7.9	26.3
4f	8	94	14.7	10.5	14.0
4g	10	92	3.8	4.4	8.6

^a From the reaction of cyclopentene oxide with TMSN₃. ^b Kinetic studies were carried out with HN₃ as the azide source (ref 4; see Supporting Information).

**Figure 3.** Initial rate kinetics for the ARO of cyclopentene oxide catalyzed by (salen)Cr complexes.

product formation using in situ IR spectroscopy.⁸ Considering a two-term rate equation involving both intra- and intermolecular components (eq 1),

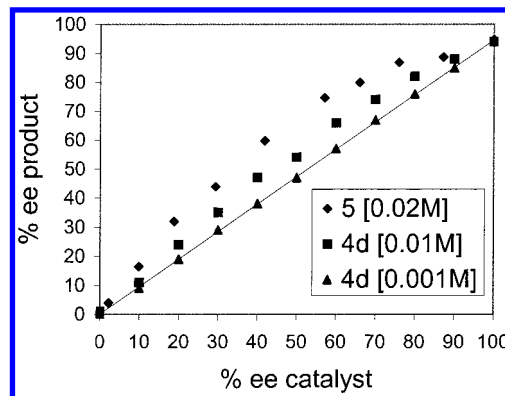
$$\text{rate} \propto k_{\text{intra}}[\text{catalyst}] + k_{\text{inter}}[\text{catalyst}]^2 \quad (1)$$

plots of rate/[catalyst] vs [catalyst] should be linear with slopes equal to *k*_{inter} and y-intercepts corresponding to *k*_{intra}. Analysis of such plots with rate data obtained with dimeric catalysts **4a–g** revealed linear correlations with positive slopes and nonzero y-intercepts, consistent with participation of both inter- and intramolecular pathways in the ARO (Figure 3). Similar analysis of rate data obtained with monomeric catalysts **1** and **5** revealed y-intercepts of zero, reflecting the absence of any first-order pathway for these catalysts.

As might be anticipated, the magnitude of the intramolecular rate constant (*k*_{intra}) measured with the dimeric catalysts displays a strong dependence on the length of the tether linking the two

(7) For example, at the 0.05 mol % level, catalyst **4c** catalyzed the complete reaction of cyclopentene oxide with TMS–N₃ within 24 h at room temperature under solvent-free conditions. Under the same conditions, catalysts **1** and **5** must be used at the 1 mol % level to effect complete reaction. With the monomeric catalysts, the reaction rate of the ARO drops off sharply with decreasing concentration, a direct consequence of the second-order dependence on [catalyst].

(8) All measurements were carried out at 23 °C with an ASI 1000 React-IR probe. Even though the reactions were kinetically well-behaved over several half-lives, initial rates were used to avoid complications arising from possible differences in the rate laws with respect to epoxide and azide between the monomeric and dimeric catalysts. Experimental procedures may be found in the Supporting Information.

**Figure 4.** Nonlinear effects in the ARO of cyclopentene oxide with TMSN₃ catalyzed by **5** and **4d**.

salen units (Table 1). With catalyst **4c** (*n* = 5), a maximum value for *k*_{intra} and enantioselectivity is obtained. With catalysts **4a,b** (*n* = 2, 4), both *k*_{intra} and enantioselectivity are reduced, presumably because the optimal transition state geometry is not accessible with the shorter tethers. The magnitude of *k*_{intra} drops progressively with catalysts **4d–g** (*n* = 6, 7, 8, 10) as well, apparently reflecting the greater entropic cost of intramolecular reaction through longer tethers. Unexpectedly, the bimolecular rate constant (*k*_{inter}) is also strongly increased by linking the catalyst units. The ratio *k*_{intra}/*k*_{inter} for a given catalyst provides a value for *M*_{eff}, a measure of the effective reactive concentration of the two salen units within the linked complexes.

A further indication of the participation of intramolecular bimetallic pathways for the dimeric catalysts was provided by examination of the dependence of reaction enantioselectivity on the enantiomeric purity of the catalysts. Monomeric catalyst **1** exhibits a distinct positive nonlinear relationship between the enantiomeric excess of product and the enantiomeric purity of catalyst,⁴ and a similar positive nonlinear effect is obtained with the monomeric catalyst **5** (Figure 4). At catalyst concentrations above *M*_{eff} (Table 1), catalyst **4d** displays an attenuated nonlinear effect, consistent with the participation of both first- and second-order pathways. However, at [4d] below the experimental value for *M*_{eff}, a strict linear relationship is observed between the ee of product and catalyst, as would be expected from exclusively intramolecular cooperative catalysis.

Covalent linkage of the (salen)Cr units of the ARO catalysts has provided catalysts 1–2 orders of magnitude times more reactive than the monomeric analogues, a fact that is remarkable considering the flexibility of the tethers that were employed to construct the dimers. Perhaps most significant, this acceleration was achieved with no loss in enantioselectivity. These results also serve to shed light on the detailed mechanism of the ARO, as the sensitivity of catalyst enantioselectivity to the position of the tether implicates a “head-to-tail” orientation in the enantioselectivity-determining transition state. Alternative linkage strategies are currently under investigation, as are mechanistic and synthetic studies of these linked catalysts in other nucleophile–electrophile coupling reactions.

Acknowledgment. This work was supported by the National Institutes of Health (GM-43214) and by postdoctoral fellowship support to J.K. from the Deutsche Akademische Austauschdienst (DAAD).

Supporting Information Available: Complete experimental procedures and characterization data for catalysts **2–5**, and details of the kinetic and nonlinear effect studies (9 pages, print/PDF). See any current masthead page for ordering information and Web access instructions.

JA982683C